Technological University Dublin
ARROW@TU Dublin

Articles | School of Mechanical Engineering

2016

Equi-biaxial fatigue testing of EPM utilising bubble inflation

Mark Johnson
Technological University Dublin

Niall Murphy
Technological University Dublin, niall.murphy@tudublin.ie

Ray Ekins
Technological University Dublin, ray.ekins@tudublin.ie

See next page for additional authors

Follow this and additional works at: https://arrow.tudublin.ie/engschmecart

 Part of the Mechanical Engineering Commons, and the Polymer and Organic Materials Commons

Recommended Citation

Mark Johnson, Niall Murphy, Ray Ekins, John Hanley, Stephen Jerrams, Equi-biaxial fatigue testing of EPM utilising bubble inflation, Polymer Testing, Volume 53, 2016, Pages 122-131, ISSN 0142-9418, DOI: 10.1016/j.polymertesting.2016.05.017.

This Article is brought to you for free and open access by the School of Mechanical Engineering at ARROW@TU Dublin. It has been accepted for inclusion in Articles by an authorized administrator of ARROW@TU Dublin. For more information, please contact arrow.admin@tudublin.ie, aisling.coyne@tudublin.ie, gerard.connolly@tudublin.ie, vera.kilshaw@tudublin.ie.



This work is licensed under a Creative Commons Attribution-NonCommercial-No Derivative Works 4.0 International License.

Authors
Mark Johnson, Niall Murphy, Ray Ekins, John Hanley, and Stephen Jerrams

This article is available at ARROW@TU Dublin: https://arrow.tudublin.ie/engschmecart/68

Test equipment

Equi-biaxial fatigue testing of EPM utilising bubble inflation

Mark Johnson*, Niall Murphy, Ray Ekins, John Hanley, Stephen Jerrams

Mechanical & Design Engineering, Dublin Institute of Technology, Dublin 1, Ireland

ARTICLE INFO

Article history:
Received 14 April 2016
Accepted 19 May 2016
Available online 21 May 2016

Keywords:
Equi-biaxial
Bubble inflation
Fatigue
Vision system
Ethylene-propylene

ABSTRACT

This paper describes an equi-biaxial tension fatigue test system which utilises the bubble inflation method to subject elastomers to equi-biaxial fatigue loading between user-defined limits of pressure, volume, stretch ratio or stress. The test system integrates a hydraulic inflation system, a high speed vision system and a control system. The high-speed vision system allows the stretch ratio and stress acting on the test specimen to be evaluated in real-time during testing. This in turn allows either stretch ratio or stress to be used as a direct control limit. In this research, constant maximum engineering stress control tests have been carried out to evaluate the suitability of the developed dynamic bubble inflation system for equi-biaxial fatigue testing of elastomers. The resulting test data was used to produce Wöhler (S/N) curves and stress/stretch ratio plots for ethylene-propylene rubber (EPM).

1. Introduction

Simple uniaxial tension is the deformation mode most often employed when conducting elastomer fatigue testing. However, in service, most elastomer components are subjected to complex multiaxial loading conditions. Biaxial fatigue testing is, therefore, more representative of actual component behaviour during service. For this reason, biaxial testing methods are necessary to obtain more accurate fatigue life predictions for elastomers in complex loading conditions, and also provide accurate material data for finite element analysis (FEA). Currently, biaxial tensile fatigue testing is not widely used as suitable test apparatus is not readily available.

As elastomer applications become more diverse, it has become increasingly important to understand their behaviour under fatigue conditions. Typical applications impose significant static and dynamic strains over long periods. For this reason, fatigue life of elastomer components is a critical issue [1].

When an elastomer is subjected to cyclic loading, it undergoes a change in stiffness and a progressive loss of mechanical strength. This change ultimately leads to crack nucleation/growth and eventual fatigue failure. Fatigue failures occur under cyclic loading where the fluctuating stress is below that of the material's ultimate tensile strength (UTS). Typically, fatigue life data for elastomers has been obtained by subjecting elastomer samples to cyclic uniaxial tension. The fatigue data is then presented using Wöhler (S/N) curves [2,3].

The international standard ISO 6943:2011 describes a standard procedure for carrying out fatigue tests on dumbbell or ring type samples using simple uniaxial tension [4]. The procedure is restricted to uniaxial fatigue tests in which the test-piece is deformed to a maximum strain and relaxed to zero strain in each fatigue cycle. There is currently no standard test method for carrying out fatigue tests using biaxial tension. However the British standard, BS 903-5:2004, guide to the application of rubber testing to finite element analysis, does outline two possible approaches for subjecting elastomers to equi-biaxial tension [5]. The first approach entails simultaneously stretching a flat sheet equally in two perpendicular directions, often achieved using a stretch frame or mutually perpendicular lead screws. The second approach involves the inflation of a flat sheet through a circular orifice, also known as bubble inflation (Fig. 1).

Stretch frames allow equi-biaxial stretch ratio values to be measured directly as the specimen geometry is a simple flat sheet. However, the frame and clamping arrangement leads to large inertia and friction losses, which are unacceptable for stress calculations when carrying out dynamic testing including fatigue testing. Bubble inflation, on the other hand, requires that equi-biaxial stretch ratio values are evaluated from a more complicated spherical/elliptical specimen geometry. However, when using bubble inflation, the effects of inertia and friction inherent in stretch frames are avoided as there are no moving mechanical parts in contact with the sample. This makes bubble inflation suitable for

* Corresponding author.
E-mail address: mark.johnson@mydit.ie (M. Johnson).

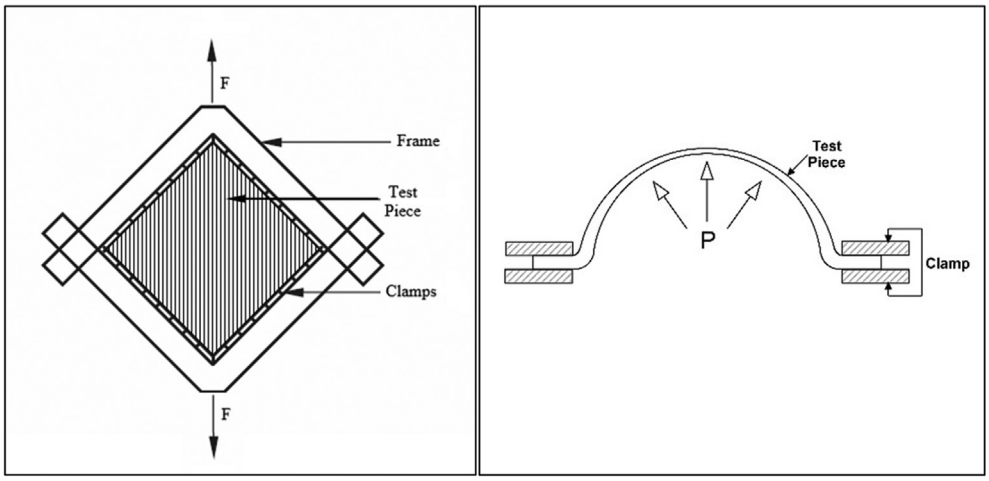


Fig. 1. Typical stretch frame design (Left), Bubble inflation (Right).

carrying out fatigue or cyclic testing. Additionally, the limitations on stretch ratio inherent in stretch frames are obviated by using bubble inflation.

This paper presents the development of a dynamic bubble inflation system, which can subject elastomers to equi-biaxial fatigue loading between user-defined limits of pressure, volume, stretch ratio or engineering stress. Previous bubble inflation systems have predominately used pressure or volume control limits, because pressure and volume can be measured directly. However, stretch ratio and stress control requires the real-time measurement of stretch ratio and stress during testing to provide control feedback. No current dynamic bubble inflation system can measure stretch ratio or stress in real-time during testing [6,7] and, as such, no current system can utilise stretch ratio or stress as a control limit. To be suitable for fatigue testing, the developed system must be capable of subjecting a sample to a comparable number of loading cycles to that of other fatigue test systems available. The resulting output data must also be in a format comparable with that of other test systems. This data must, therefore, take the form of stress/stretch ratio plots and Wöhler curves.

Constant maximum engineering stress control fatigue tests have been conducted in this study on Ethylene-Propylene rubber (EPM) samples to evaluate the suitability of the developed dynamic bubble inflation system for long-term equi-biaxial fatigue testing. The resulting test data is presented in the form of stress/stretch ratio plots and a Wöhler curve.

2. Bubble inflation

Bubble inflation is considered to comply with theory for applying pressure to a thin shell structure that possesses negligible bending stiffness, alternatively described as membrane theory. For an ideal isotropic material and an axisymmetric set-up, the bubble contour behaves with rotational symmetry and,therefore, the deformation and stress at the bubble pole region is equi-biaxial [8,9].

A thin sheet, of thickness t_0, is clamped above a circular inflation orifice. Pressure, P, is applied to one side of the thin sheet to produce a bubble shell (Fig. 2). From the measurement of pressure, P, the radius of curvature, r and the stretch ratio, λ, the nominal or engineering stress in the pole region can be determined using Eq. (1) [7].

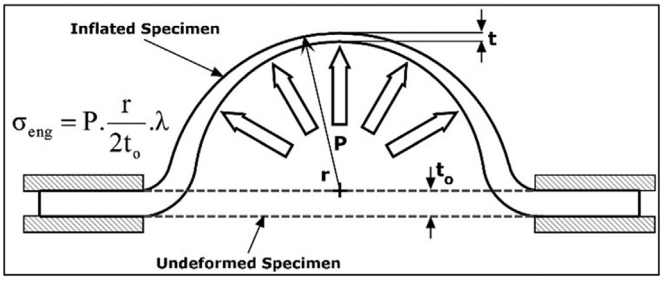


Fig. 2. Bubble inflation.

$$\sigma_{eng} = P \cdot \left(\frac{r}{2t_o}\right) \cdot \lambda \tag{1}$$

where: σ_{eng} = engineering stress (MPa or N/mm^2), P = applied pressure (MPa), r = radius of curvature (mm), t_o = original sheet thickness (mm) and λ = equi-biaxial stretch ratio in the pole region.

2.1. Single shot bubble inflation

Many researchers have developed bubble inflation systems capable of observing material behaviour during a single inflation cycle (single shot) [6,8–12]. Such systems solely provide equi-biaxial stress-stretch ratio data for a single inflation cycle or for a small numbers of manually controlled inflation cycles. Early bubble inflation systems such as that developed by Treloar [10] required manual measurements to be taken at different intervals throughout inflation. Recent systems have utilised vision systems with great success to evaluate the stretch ratio and stress experienced by elastomer bubble samples [8,9,11,12]. Reuge [11] and Johannknecht [8] realised the potential of utilising vision systems and stated that, with further development, dynamic fatigue testing may be possible if high speed vision systems with sufficient image processing speeds were utilised.

2.2. Dynamic bubble inflation

Two systems have been identified which observe material behaviour during dynamic or cyclic inflation. Hallett [6] developed a dynamic bubble inflation system capable of subjecting elastomers to equi-biaxial fatigue loading using inferred stretch ratio as a

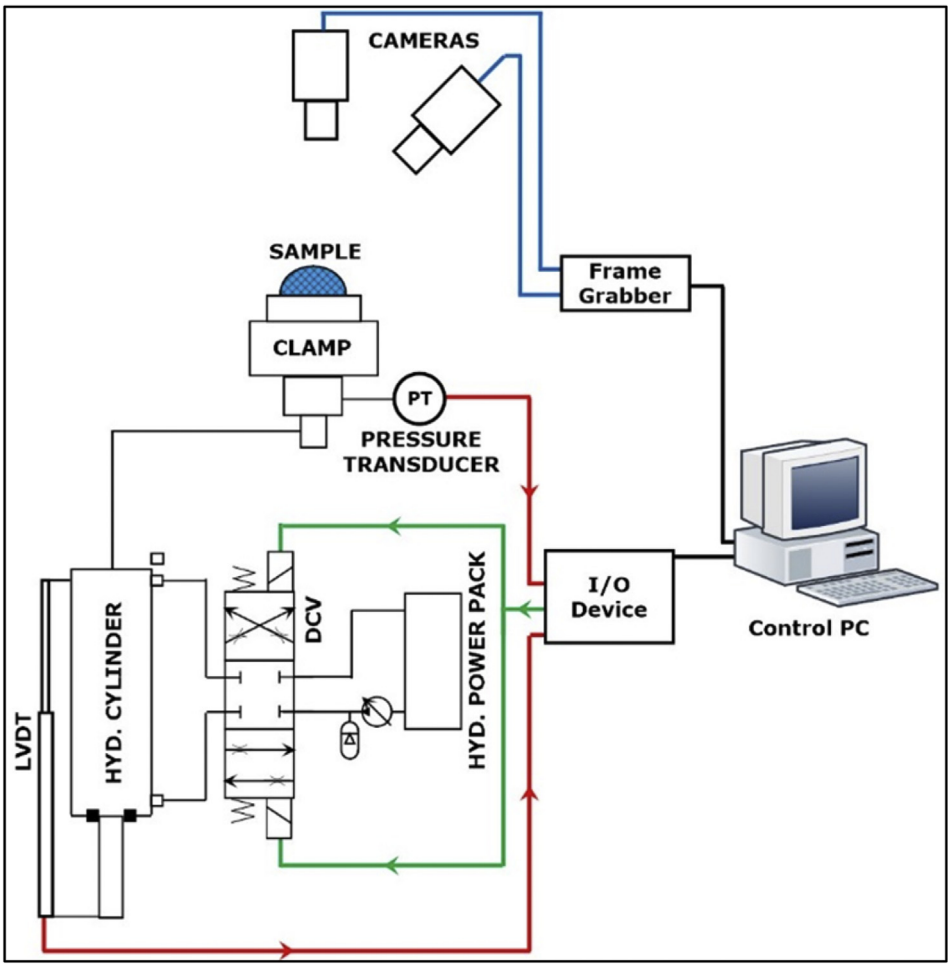


Fig. 3. Biaxial fatigue test system schematic.

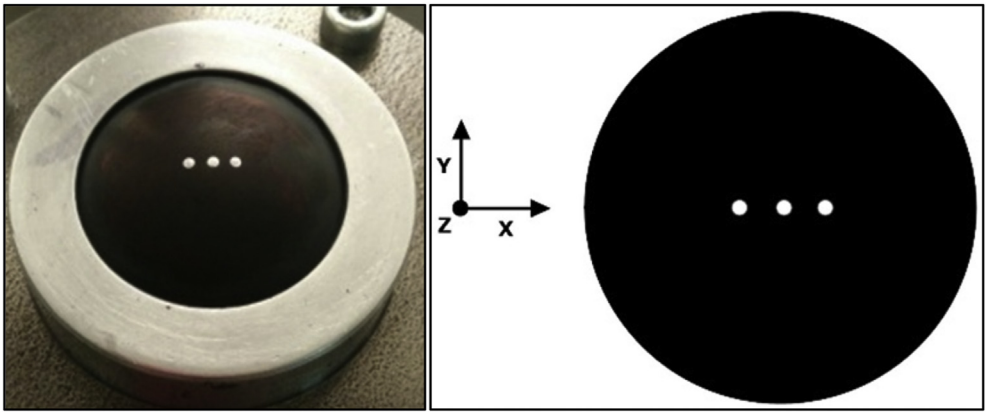


Fig. 4. Elastomer specimen with dot markings (Left), Digital representation (Right).

control limit. During testing, samples were inflated repeatedly to pre-set heights dictated by a limit switch comprising a light metal flap and a pneumatic sensor. Hallett's bubble inflation system did not take direct measurements of stretch ratio and stress acting within the inflated bubble pole region. Local strains were inferred from measured bubble height values alone. This is at odds with Johannknecht [8] who stated that the evaluation of local strains cannot be made from bubble shape or height.

Murphy et al. [7,13] developed a dynamic bubble inflation system capable of subjecting elastomers to equi-biaxial fatigue loading using either constant maximum pressure, volume or inferred engineering stress as a control limit. During fatigue testing, a vision system captured stereo pair images at a rate of 29 Hz. These images were post processed to calculate the radius of curvature and the stretch ratio within the bubble pole region once testing was complete. As the pressure acting on the sample was recorded during

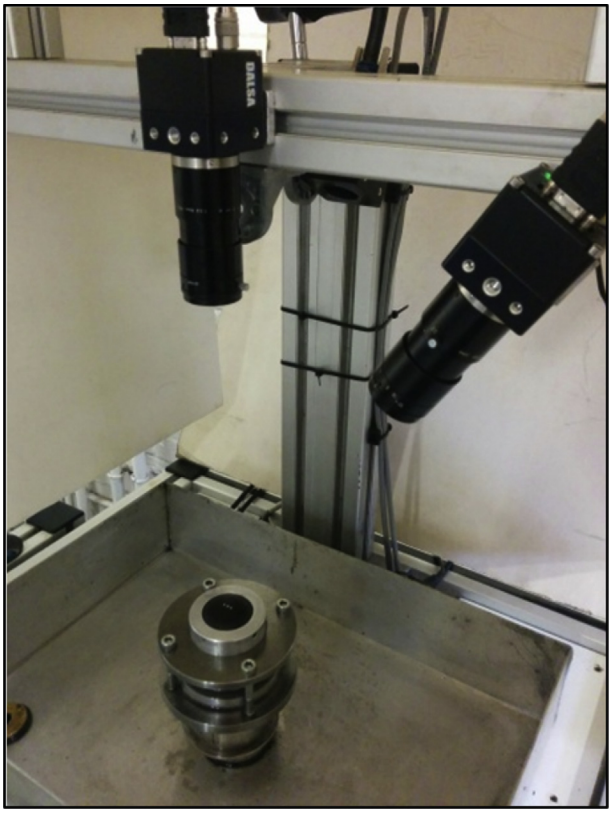


Fig. 5. Camera orientation.

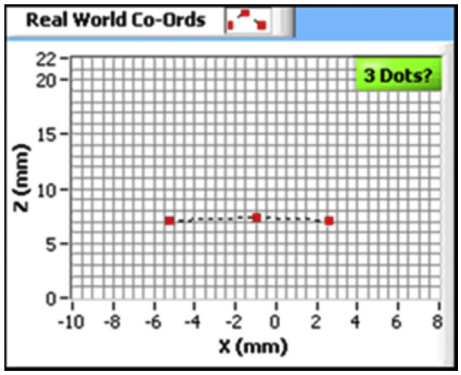


Fig. 7. Example calculated X, Z real-world coordinates.

To achieve inferred engineering stress control, Murphy created reference tables by experiment which provided the radius of curvature and stretch ratio for different volumes of inflation. Using these reference tables, the measured pressure and the original thickness of the material, engineering stress control could be achieved without requiring direct measurement of the radius of curvature and stretch ratio.

Currently, no long-term dynamic bubble inflation system can evaluate the stretch ratio and stress within the bubble pole region in real-time during testing. As such, it is also true that no dynamic bubble inflation system can subject elastomers to cyclic fatigue loading using direct stretch ratio or stress control limits.

2.2.1. Utilising a high speed vision system for dynamic bubble inflation

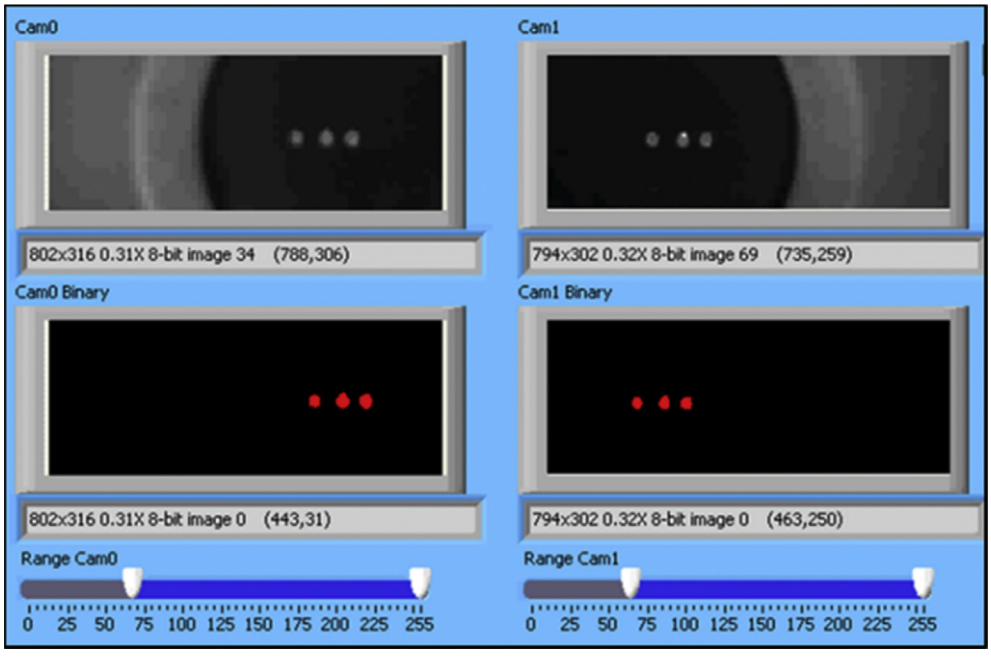


Fig. 6. Image thresholding, Top: original acquired images, Bottom: binary images.

testing and the original thickness of the material known, the stress acting within the bubble pole region could also be calculated post process. Although Murphy's system provided stretch ratio and stress measurements, they could not be used to give direct control feedback as they were calculated post-process and not in real-time.

To allow stretch ratio or stress to be utilised as a control limit, real-time measurement of the radius of curvature and stretch ratio in the bubble pole region is required along with the pressure acting on the bubble sample. Using a real-time system, stretch ratio or

stress, calculated using Eq. (1), can be utilised to provide direct control feedback. Pressure can be measured directly using a pressure transducer. However, radius of curvature and the stretch ratio measurements prove more difficult as a non-contact measurement system is required. Previous authors [7–9,12] have successfully used vision systems to take these measurements, but this has either occurred post-process or at image processing speeds too slow to provide adequate control during dynamic testing. The bubble inflation system outlined in this work utilises a high-speed vision system to record radius of curvature and stretch ratio measurements in the bubble pole region in real-time during testing.

A number of conditions are required if a high-speed vision system is to be utilised to measure the radius of curvature and stretch ratio during dynamic bubble inflation. One requirement is maintaining image contrast. Markings must be made on the bubble sample's surface in order to provide points of reference from which the vision system can record measurements. Markings must be of contrasting colour to that of the sample background to allow the vision system to detect them. It is critical that image contrast is maintained during testing to ensure all markings are detected correctly, thus avoiding measurement errors. Background lighting has a direct effect on image contrast. Typical vision applications target a stationary object with fixed geometry. However, as a bubble sample inflates and deflates, its surface geometry continuously changes and, as such, the angle at which incoming light hits the bubble surface also changes. This can lead to 'bright spots' on the bubble surface, which can cause part of the image sensor to become over exposed, resulting in a loss of image contrast.

Another consideration is image processing which is required in order to evaluate measurements using the acquired images from a vision system. Image processing is computationally intensive. This is not problematic if carried out post-process over an extended period. However, if real-time image processing is required, a large proportion of the test system's processing capacity must be utilised in order to complete the task within the allotted time. Any additional calculation, data display, data logging or control operations performed in parallel, place a further load on the processor. If the test system is to be utilised to carry out fatigue tests, it must be capable of carrying out tests of comparable duration to that of other fatigue testing methods. This requires the development of a control system and control software that can operate for the duration of a fatigue test. To achieve this, careful consideration must be given to reducing processor loads where possible when developing control system software.

3. Dynamic bubble inflation system development

The test system developed for this study utilises the bubble inflation method to subject elastomer samples to equi-biaxial fatigue loading. It consists of an inflation system, a vision system and a control system. A schematic view of the test system can be seen in Fig. 3. Fatigue tests can be carried out between user-defined limits of pressure, volume, stretch ratio or stress.

3.1. Inflation system

The inflation system was developed to hydraulically inflate and deflate an elastomer bubble specimen at a rate of up to 1 Hz and to a maximum inflation pressure of 10Bar. A rate of 1 Hz was chosen as it is within the range suggested by ISO 6943:2011 [4] for an elastomer tension fatigue testing machine. This rate of inflation/deflation ensures excessive heat build-up (thermal runaway) within the

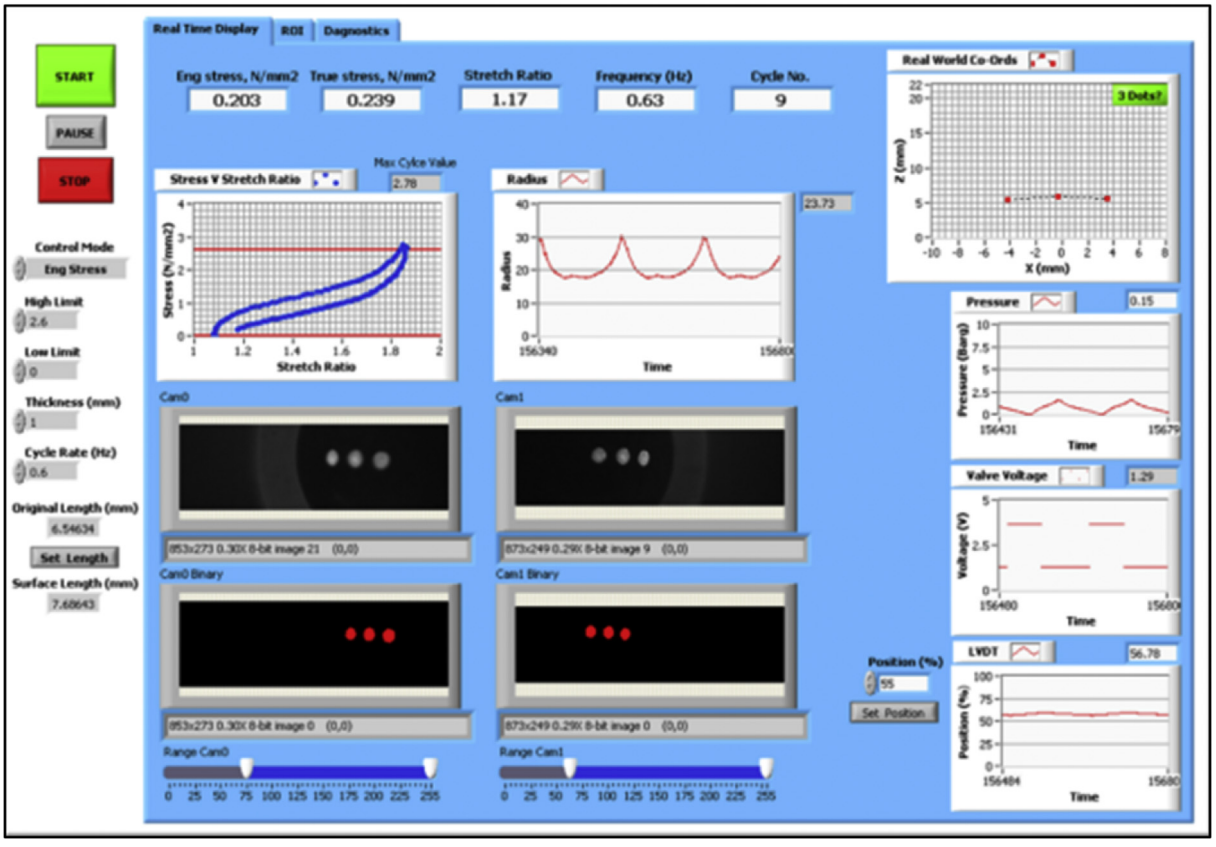


Fig. 8. Overview of test system GUI.

Table 1
Performance specifications.

Test system performance specifications	
Control modes	Volume, pressure, stretch ratio, engineering stress & true (Cauchy) stress
Max. inflation pressure	10 Bar
Max. stretch ratio, λ	3.5 (Higher achievable, dependant on camera set-up)
Max. cycle rate	1 Hz (ISO 6943:2011)
Vision system frame rate	120 fps
Vision system resolution	0.04 mm/pixel (Resolution improves as sample inflates)
Image processing rate	100 Hz (10 ms)
Data acquisition rate	100 Hz (10 ms)

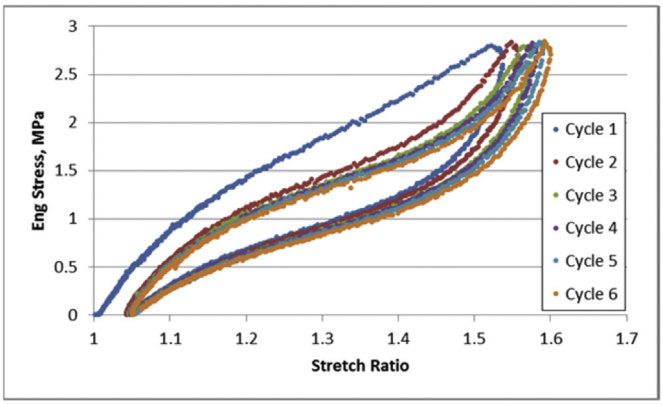


Fig. 9. Example pre-conditioning cycles, max $\sigma_{eng} = 2.8$ MPa.

sample is prevented, allowing thermal degradation to be excluded as a potential cause of sample failure.

A circular clamp with a 35 mm inflation orifice is used to clamp a 50 mm diameter sample around its periphery. To inflate the sample, a hydraulic cylinder is employed. Hydraulic pressure is supplied by a hydraulic power pack via a proportional directional control valve (DCV) to achieve reciprocating motion. A pressure transducer is used to measure the inflation pressure acting on the bubble sample and a linear variable displacement transducer (LVDT) measures the cylinder's position during inflation cycles.

3.2. Vision system

The vision system allows the non-contact measurement of the stretch ratio and the stress acting in the bubble pole region in real-time during cyclic inflation. For an isotropic material, the stretch ratio and stress in the pole region are equi-biaxial. Therefore, measurements recorded in one axis alone are sufficient to provide the equi-biaxial stretch ratio and stress. To facilitate these measurements, the real-world coordinates of three dot markings, made along the X-axis, within the bubble pole region of the specimen (Fig. 4) are evaluated.



Fig. 10. Example single shot test sample after failure.

Two CMOS cameras with a resolution of 1024 × 1024, a frame rate of 120fps and 50 mm lenses are utilised. The cameras are placed in a stereo vision configuration with a clear view of the elastomer sample (Fig. 5). The spatial resolution of the cameras at a working distance of 230 mm is approximately 0.04 mm/pixel. This improves during testing, as a sample will approach the cameras when inflated.

During inflation cycles, images from the vision system are acquired and processed in real-time by the control system outlined in Section 3.3. To reduce processing loads, the size of the acquired images is made smaller by adjusting the region of interest (ROI) to exclude the vision area which the dots do not transverse during inflation. To maximise contrast between the dots and sample background, a suitable marking colour is chosen. To prevent loss of contrast due to 'bright spots' on the sample surface, diffuse lighting is utilised. Image thresholding is used to convert acquired images to binary images, highlighting the contrast between the dots and the sample surface (Fig. 6).

Particle analysis utilising 8-pixel connectivity is used to provide the pixel coordinates of the centroid of each dot within the created binary images. Using the centroid pixel coordinate of matching stereo pairs and a 3D camera calibration, the X, Z real world coordinates of the dots on the bubble samples surface are calculated (Fig. 7).

Once the real-world X, Z coordinates are calculated, mathematical relationships can be used to evaluate the radius of curvature, r and the surface length, l, between the outer most dots on the bubble sample surface. The bubble surface stretch ratio, λ, in the pole region can then be calculated using Eq. (2).

$$\lambda = \frac{l}{l_o} \tag{2}$$

where: λ = the equi-biaxial stretch ratio in the pole region, l = final surface length (mm) and l_o = original surface length (mm).

Once the radius of curvature, r and stretch ratio, λ, have been calculated, the engineering stress, σ_{eng}, acting in the pole region can be calculated using Eq. (1), as the original thickness, t_o, of the sample is already known and the applied pressure, P, is measured using the inflation system's pressure transducer.

3.3. Control system

The control system monitors and controls the inflation and vision systems. It consists of a PC running proprietary control and data acquisition software (LabVIEW), a data acquisition module and

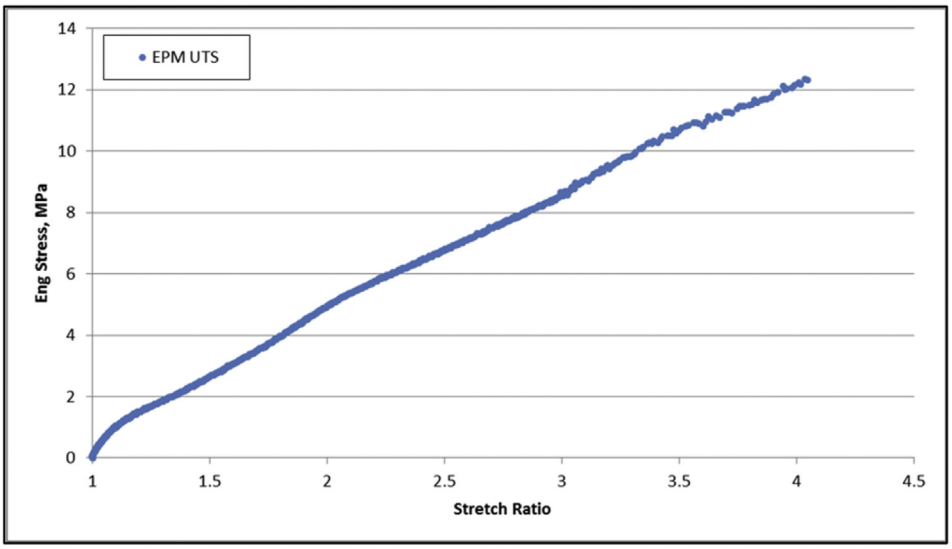


Fig. 11. EPM single shot test stress/stretch ratio plot.

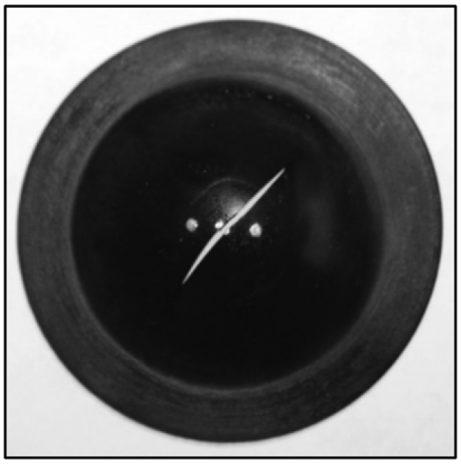


Fig. 12. Example fatigue test sample after failure.

a frame grabber.

The developed software controls inflation cycles between user-selected limits of pressure, volume, stretch ratio, engineering stress or true stress. This allows a control method to be chosen which provides the most accurate representation of the loading conditions experienced by a component during service. During testing, all image processing is carried out as described in Section 3.2. Calculated stress and stretch ratio data within the pole region is monitored and logged in real-time. A graphical user interface (GUI), provides a control interface and displays all relevant test data (Fig. 8).

Experimental data is logged every 10 ms and can be extracted once testing has finished. Using extracted experimental data, stress-stretch ratio plots can be created by plotting stress values against corresponding stretch ratio values for any fatigue cycle. If desired, multiple stress-stretch ratio plots can be placed on a single graph. Wöhler (S/N) curves are created by combining the results of many fatigue tests of the same material at different maximum loading values. This is achieved by plotting the maximum control limit against the number of cycles required to cause failure for each test. Key test system performance specifications are listed in Table 1.

4. Materials and method

70 IRHD Ethylene-Propylene rubber (EPM) was used for all tests in this study. Test samples consisted of 50 mm diameter, 1.1 mm thick EPM discs. Samples were clamped over the inflation orifice of the test rig and inflated using a hydraulic fluid that would not induce sample swelling [14]. Inflation fluids can be selected independently of the hydraulic power pack's fluid to ensure compatibility with the elastomer under investigation. Two types of testing were carried out; equi-biaxial static (single shot) tests and equi-biaxial fatigue tests.

Single shot tests were carried out to establish the UTS of the EPM. This was achieved by inflating a sample until failure occurred. The stress and stretch ratio acting in the pole region was monitored and recorded throughout inflation.

Equi-biaxial fatigue tests were carried out between pre-defined engineering stress limits. During fatigue testing, samples were cycled between a maximum upper engineering stress and a stress of zero until failure occurred. The number of cycles required to reach failure was noted for each test. Three samples were tested for each maximum stress limit used, in order to establish an average number of cycles to failure.

All fatigue test samples were preconditioned before testing. Preconditioning was achieved by cycling the sample six times to its intended maximum stress control limit (Fig. 9).

This is the minimum number of preconditioning cycles recommended by ISO 4664-1:2011 [15] when carrying out dynamic testing on elastomers. After these cycles, the sample was unloaded and the stretch ratio was reset to a value of one. Preconditioning in this way is especially useful in the bubble inflation case when testing samples that exhibit significant levels of set. Set or residual deformation leads to the formation of a measurable radius of curvature at a stress of zero, which allows the stress acting within the pole region to be calculated with greater accuracy at low stretch ratios.

5. Results and discussion

5.1. Equi-biaxial single shot tests

Fig. 10 shows the rupture pattern of a single shot sample after testing; it is noted that the sample exhibits multiple tears which

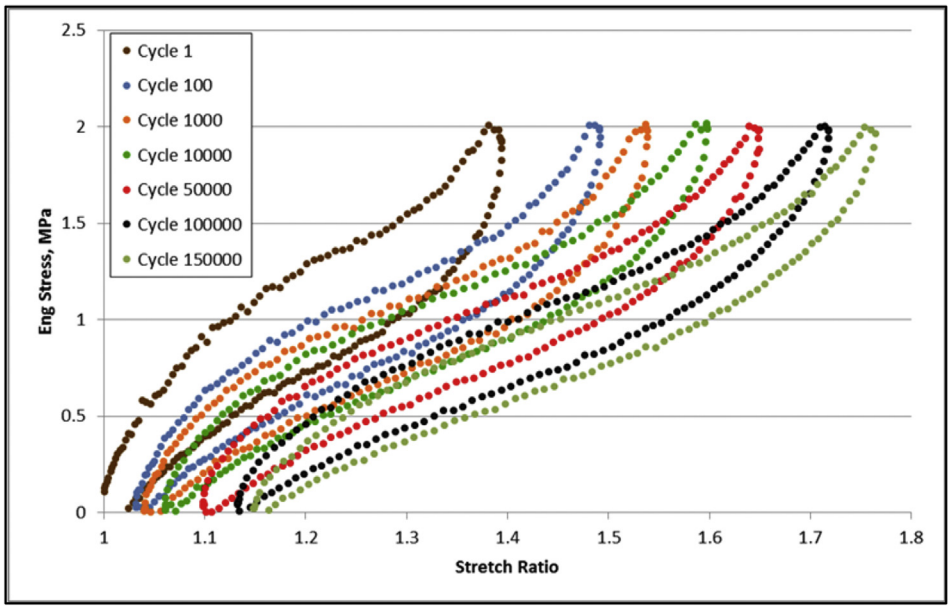


Fig. 13. Selected engineering stress-stretch ratio plots from fatigue test, max $\sigma_{eng} = 2$ MPa.

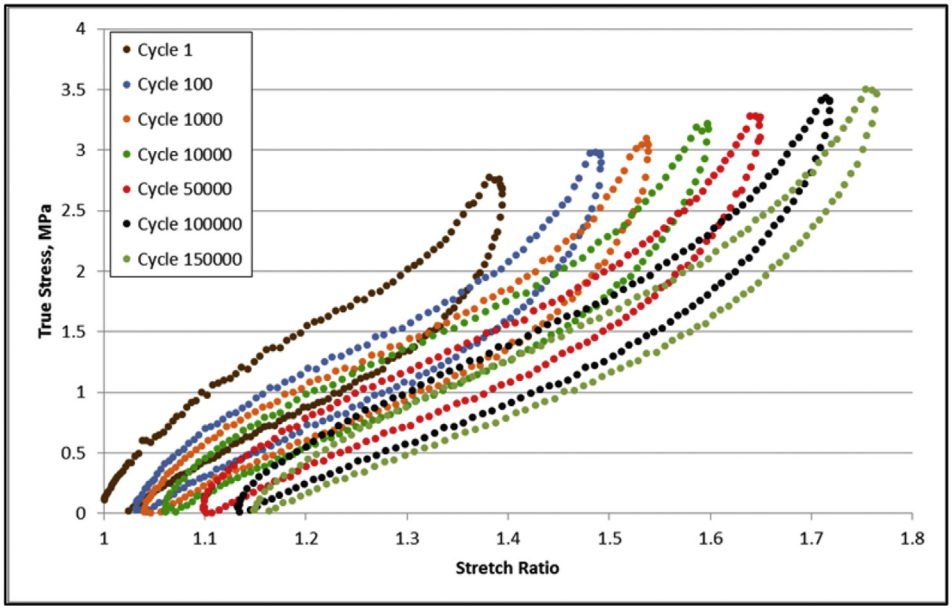


Fig. 14. Selected true stress-stretch ratio plots from fatigue test, max $\sigma_{eng} = 2$ MPa.

radiate from its pole, the point of maximum stress. This type of failure is typical of samples which have undergone single shot testing using hydraulic bubble inflation [16].

Fig. 11 shows the stress/stretch ratio plot recorded for a single shot test. It can be seen that the stress at which failure occurs, and hence the equi-biaxial UTS of the EPM material used, is approximately 12.3 MPa. Using this UTS value, an appropriate stress range for the equi-biaxial fatigue test programme was selected.

5.2. *Equi-biaxial fatigue tests*

Fig. 12 shows the rupture pattern of a fatigue sample after testing; it is noted that the sample exhibits a single tear, which crosses the pole region. This type of failure is typical of samples that have undergone cyclic fatigue testing using hydraulic bubble inflation [16]. The tear propagates from the pole region as this is where the maximum principal stress occurs. This is an advantage when compared with other equi-biaxial tension methods as often, for other methods, sample failure occurs at the clamping interface due to large stress concentrations which exceed that of the stress acting in the region of interest (the centre of the test piece). If a tear occurs outside the pole region, it is an indication that failure has occurred due to a significant material flaw as it has failed in a region which has been subjected to lower stress than that of the pole region. A small number of fatigue tests that resulted in a tear outside the pole region were discarded.

Every fatigue test carried out also provided stress-stretch ratio plots for each cycle. Selected stress/stretch ratio plots from a typical

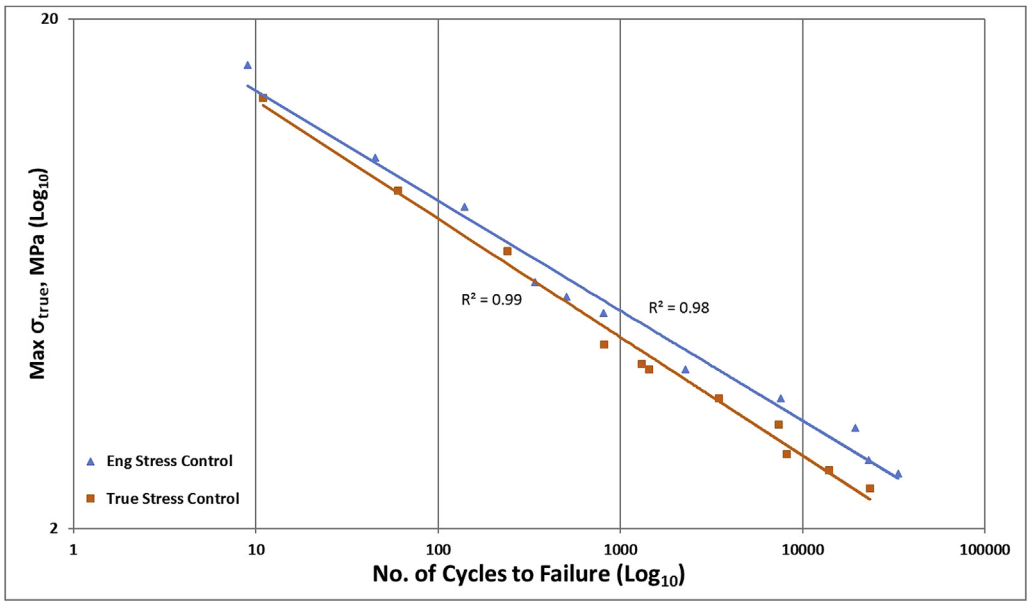


Fig. 15. Comparison of true stress and engineering stress control.

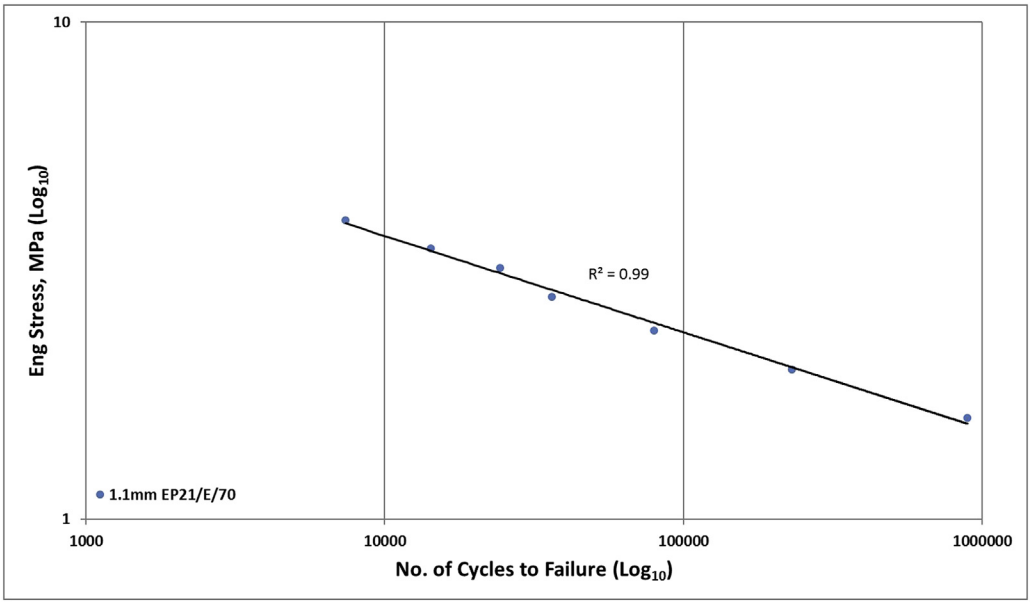


Fig. 16. EP 75 Wöhler curve.

fatigue test can be seen in Fig. 13. It is clear that, as the test progresses, continuous stress softening occurs for this material. However, the rate at which stress softening occurs falls off as the number of cycles increase.

The tests undertaken in this study were carried out using maximum engineering stress control limits. As elastomers experience large deformations when loaded, engineering stress does not accurately represent the actual stress acting on the material. Fig. 14 shows the actual true stress experienced by the sample during the same fatigue test shown in Fig. 13. The true stress continuously increased as the stretch ratio increased; this is due to the reducing cross sectional area of the sample as the test progressed and stretch ratio increased.

Although engineering stress does not provide a perfect representation of the true stress experienced by an elastomer, it does lend itself to comparing the fatigue performance of different elastomers. In a previous study carried out by the authors, a comparison was made between maximum true stress and maximum engineering stress control [17]. If the same initial test conditions are considered, utilising maximum engineering stress as the control limit leads to earlier sample failure than that using maximum true stress control. This is shown in Fig. 15, which is a plot of the number of cycles to failure for each control method against the initial or starting true stress for each sample. Therefore, using engineering stress control allows the fatigue performance of different elastomer materials to be compared in a shorter time frame. However, true stress control can be implemented if a specific true stress value is desired at sample failure.

The results of the equi-biaxial fatigue testing carried out in this study are presented in the format of a Wöhler curve, shown in Fig. 16. As expected, the numbers of cycles required to cause sample failure increased as the maximum engineering stress limit decreased. It can also be seen that the number of fatigue cycles achieved is in excess of 800,000.

The Wöhler curve can be used to establish an equation which defines the fatigue performance of the tested material. Therefore, the fatigue performance of the EPM tested in this study when subjected to a constant maximum engineering stress is given by Eq. (3).

$$N_f = 8.445 \times 10^6 \sigma_{eng}{}^{-5.13} \quad (3)$$

By substituting σ_{eng} with any maximum stress limit, the approximate number of cycles to failure (N_f) can be calculated.

6. Conclusions

The results presented demonstrate that the developed dynamic bubble inflation system can be utilised to carry out equi-biaxial fatigue testing on elastomer samples. Single shot and equi-biaxial fatigue tests have been successfully carried out on EPM samples using the test system. The rupture patterns observed are similar to that observed in previous studies utilising hydraulic bubble inflation [8,16]. The results of the equi-biaxial fatigue tests are in the form of stress-stretch ratio plots and a Wöhler curve. The Wöhler curve allows the fatigue life of EPM subjected to any constant maximum engineering stress to be determined. The number of fatigue cycles achieved during this study, in excess of 800,000, are comparable to that of other test systems utilised to study elastomer fatigue and exceed that of the dynamic bubble inflation system developed by Murphy et al. [6,13,18,19]. This demonstrates that the control system and software developed can operate reliably despite the intensive computational requirements for image processing and the issues outlined in maintaining image contrast. The stress-stretch ratio plots demonstrate the test system's ability to record stretch ratio and stress acting in the bubble pole region during testing. This is achieved in real-time using a high-speed vision system. The stress-stretch ratio plots also demonstrate the test systems ability to maintain maximum engineering stress control limits throughout testing, using real-time measurements of stress to provide direct control feedback. True stress, stretch ratio, pressure or volume control is also possible. Engineering stress control allows the fatigue performance of different elastomer materials to be compared in a shorter time frame when compared to other control methods.

The test system can be utilised to compare the fatigue performance of many different elastomers under equi-biaxial tension, facilitating the design of elastomer components for maximum fatigue life. The stress and stretch ratio plots taken during testing can also be used to establish constants required to carry out FEA analysis. This facilitates the detailed analysis of elastomer at different stages of service life. Further work in the area could lead to the development of an ISO standard for the determination of equi-biaxial tension fatigue, using dynamic bubble inflation, or alternatively lead to its inclusion in ISO 6943 [4].

References

[1] W.V. Mars, A. Fatemi, A literature survey on fatigue analysis approaches for rubber, Int. J. Fatigue 24 (2002) 949–961.
[2] S.M. Cadwell, R.A. Merrill, C.M. Sloman, F.L. Yost, Dynamic fatigue life of rubber, Ind. Eng. Chem. Anal. Ed. 12 (1940) 19–23.
[3] J.H. Fielding, Flex life and crystallization of synthetic rubber, Rubber Chem. Technol. 17 (1944) 398–403.
[4] ISO 6943, Rubber, vulcanized, in: Determination of Tension Fatigue, 2011.
[5] BS 903-5, Guide to the Application of Rubber Testing to Finite Element Analysis, 2004.
[6] J. Hallett, Multiaxial Strength and Fatigue of Rubber Compounds, PhD Dissertation, Loughborough University, United Kingdom, 1997.
[7] N. Murphy, Providing Stress Controlled Equi-biaxial Fatigue Test Data for Elastomers Using the Bubble Inflation Method, PhD Dissertation, Dublin Institute of Technology, Ireland, 2009.
[8] R. Johannknecht, G. Clauss, S. Jerrams, Determination of non-linear, large, equal biaxial stresses and strains in thin elastomeric sheets by bubble inflation, Proc. Inst. Mech. Eng. Part L J. Mater. Des. Appl. 216 (2002) 233–243.
[9] P.H. Mott, C.M. Roland, S.E. Hassan, Strains in an inflated rubber sheet, Rubber Chem. Technol. 76 (2003) 326–333.
[10] L.R.G. Treloar, Strains in an inflated rubber sheet, and the mechanism of bursting, Rubber Chem. Technol. 17 (1944) 957–967.
[11] N. Reuge, F.M. Schmidt, Y. Le Maoult, M. Rachik, F. Abbé, Elastomer biaxial characterization using bubble inflation technique. I: experimental investigations, Polym. Eng. Sci. 41 (2001) 522–531.
[12] J. Javorik, Z. Dvorak, Equibiaxal test of elastomers, Kautsch. Gummi Kunstst. 60 (2007) 456–459.
[13] N. Murphy, J. Hanley, S. Jerrams, The effect of pre-stressing on the equi-biaxial fatigue life of EPDM, in: Constitutive Models for Rubber VI, CRC Press, United Kingdom, 2009.
[14] J. Hanley, Swelling effects in dynamic equi-biaxial testing of EPDM elastomers by the bubble inflation method, PhD Dissertation, Dublin Institute of Technology, Ireland, 2008.
[15] ISO 4664-1, Rubber, vulcanized or thermoplastic, in: Determination of Dynamic Properties, 2011.
[16] N. Murphy, J. Hanley, J. McCartin, B. Laningan, S. McLoughlin, S. Jerrams, G. Clauss, R. Johannknecht, Determining multiaxial fatigue in elastomers using bubble inflation, in: P.-E. Austrell, L. Kari (Eds.), Constitutive Models for Rubber IV, CRC Press, United Kingdom, 2005, pp. 65–70.
[17] M. Johnson, J. Hanley, S. Jerrams, R. Ekins, N. Murphy, Constitutive models for rubber VIII, in: N.G.N. Laborda, A. Alonso (Eds.), Constitutive Models for Rubber VIII, CRC Press, United Kingdom, 2013, pp. 383–386.
[18] F. Abraham, T. Alshuth, S. Jerrams, The effect of minimum stress and stress amplitude on the fatigue life of non strain crystallising elastomers, Mater. Des. 26 (2005) 239–245.
[19] T. Zarrin-Ghalami, A. Fatemi, Multiaxial fatigue and life prediction of elastomeric components, Int. J. Fatigue 55 (2013) 92–101.